An advanced identification procedure for material model parameters based on image analysis

An advanced identification procedure for material model parameters based on image analysis

Lorenzo Peroni, Martina Scapin, Claudio Fichera

Department of Mechanical and Aerospace Engineering, Politecnico di Torino

1 Abstract

Inverse methods for the material strength model calibration are widespread techniques, which allow taking into account for the actual strain, strain-rate, temperature and triaxiality fields inside the specimen. An optimization procedure generally starts from experimental measurement of force-stroke time history and is based on the minimization of the difference between experimental and numerically computed quantities.
In this work, the strength model identification is performed also on the basis of the specimen shape recorded during the test. This information is imposed as boundary condition, which forces the experimental profile to the external surface of the specimen. The optimization is based on the minimization of the reaction force of the imposed boundary condition. This technique could be applied both to quasi-static and dynamic tests, also at different temperatures, since the only additional requirement is a video of the test with a good compromise in terms of spatial and time resolutions. The methodology is compared with a standard numerical optimization procedure, in order to evaluate the reliability of the method and the advantages/disadvantages of this new approach.

***KEYWORDS: inverse method, digital image analysis, specimen deformation, contact force, multi-objective-optimization**

2 Introduction

Nowadays, Finite Element (FE) simulations are a valid and widespread tool used in the design phase in several fields as well as in the understanding of complex phenomenon allowing, in some cases, the limitation of full-scale experimental tests, which could be dangerous and expensive. The reliability of the numerical results are strongly dependent from the chosen constitutive model and its parameters, which have to be properly determined. The tensile test is often considered for the material model identification. In case of ductile metals and alloys, for which large strains can be reached before fracture, the data analysis at the basis of identification process has to be carefully treated. At small strains (in elastic and nearly plastic regime), the specimen deforms homogenously both along cross section and gage length. The longitudinal strain can be calculated, using strain-gages, extensometer or digital image correlation, as the engineering one (ratio between the stroke and the initial gage length) or as the logarithmic one. The value obtained is equal to the equivalent strain. Accordingly, also the uniaxial stress can be derived and used as the equivalent stress. After the maximum of the engineering stress is reached, the presence of geometrical instability and the localization of necking produce a complex triaxial state of stress characterized by large strains. In this regime, the longitudinal strain has to be actualized with respect to the portion of the specimen in which the deformation is localized: the estimation of the effective strain can be performed by measuring the actual diameter of the minimum cross section. On the other hand, the determination of the equivalent stress, which is no longer equal to the uniaxial one, is more complicate. Commonly, in the scientific literature, different approaches are used to solve this problem: analytical methods, iterative numerical inverse procedures based on FE simulation and Virtual Field Methods (VFM).

2.1 State-of-the-art

The analytical methods implies the definition of mathematical relations for the estimation of the equivalent stress starting from the nominal stress and the geometry of the necking region (such as the minimum cross section and the radius of the curvature of the necking profile). In this sense, the first solution was proposed by Bridgman in [1] for round specimen and later by [2] for rectangular cross-section specimens. The objective was to determine the correction factor to extend the validity of the logarithmic stress after instability occurs. In the scientific literature, several researchers applied the Bridgman equation to obtain the effective stress-strain relation of the material, as for example in [3-5]. It is well recognized that the Bridgman model has some limitations, especially due to the fact that it

predicts a uniform distribution of the stress over the minimum cross-section. This was demonstrated, for example in [6], in which the Bridgman prediction was compared with FE results. In order to overcome the limitation of the Bridgman model, other researchers proposed modified formulations, as in [7], in which the author derived a new material-independent model for the necking problem, named MLR model.
Some authors proposed an alternative method for the description of the post-necking behavior based on full-field measurements combined with Virtual Field Methods. A lot of works can be found, in which the VFM was applied to the elastic behavior of material. For non-linear description (such as plasticity, visco-plasticity and damage), it is not possible to find an explicit relation between stress and strain and, consequently, an iterative procedure is needed. The first application to the model identification in case of elasto-plastic constitutive relation was performed in [8] and recently extended to large plastic deformation in [9-10]. In [11], a new inverse technique is proposed for thin sheet. The method is based on full-field strain measurements and only requires a stress update algorithm, on the basis of the minimization of the discrepancy between internal and external work in the necking region. In few works, such as in [12-13], a rate-dependent model was used for the identification of the strain-rate sensitivity of the materials under investigation.
The majority of the approaches used for the constitutive model identification are based on iterative numerical inverse methods, in which the target function is the minimization of the difference between experimental and numerically computed quantities. The satisfaction of the optimization criteria is obtained by changing the strength model parameters in FE simulations. The major drawbacks of this technique are related to the reliability in the FE model construction and the high computational costs. On the other hand, the main advantage is that no hypothesis on the internal distribution of the mechanical quantities is required with respect to their measurements on the specimen surface. Some of the most recent works, in which this technique is used are [14-15].
One limitation of this technique is that the model identification is obtained by fitting the macroscopic quantities (such as force and displacement) while there are not any constraints on the specimen deformation. In some cases, as for example in [16], the at the end of the optimization process, the numerical and the experimental profiles of the deformed specimens are compared, but this information is not used during the optimization process.
In case of dissimilarities between the numerical and the computed deformed profiles, the problem could be solved by performing again the numerical optimization but changing, for example, the set of considered experimental targets or their relative weights, the set of material model parameters considered as optimization variables and the used strength model. Obviously, this procedure is highly time-consuming and the achievement of satisfactory results is not guaranteed.

3 Advanced numerical inverse method

In this perspective, in this work, an advanced FE-based numerical inverse procedure is proposed, with the idea of taking under control also the specimen deformation. The method is based on the digital image analysis of the recorded sequence of the specimen deformation.
This approach finds application also in high dynamic tests, in which, in some cases, the direct measurements of force and displacement can be complicated or even impossible due to noise, inertia phenomena, resonance of the measuring system, etc. On the other hand, it could be simpler to record the deformation process with high speed camera (or high resolution camera in quasi-static tests).
With the aim to take into account the specimen deformation during the material model identification process, a solution could be to constrain the specimen deformation on the basis of information, extracted from the experimental test, such as the minimum section, the radius of the necking area, the level of triaxiality, etc. At this stage two problems arises.
The first one is related to the fact that, as previously mentioned, this approach requires the recording of the whole deformation process and, consequently, an accurate image elaboration. In this sense, first of all, it is needed to record images with a good compromise in terms of spatial and time resolutions. After that, the data elaboration should be able to precisely identify the specimen profile and its modification during the deformation.
The second problem is how to practically introduce these information in a FE-based inverse optimization procedure. As a matter of fact, in several commercial code, such as in LS-DYNA, this type of data is not automatically extracted from the simulation. This means that they can not be used in a standalone optimization program, such as LS-OPT, but they require to write user defined routines or to interface the FE solver with an external optimization tool.
In order to avoid these solutions, the authors propose to define a second part in the FE model, which is able to impose the correct (experimental) deformation to the external profile, by interacting with the

specimen. This second part represents a sort of “Reference Shape” (labeled as RS in the following), which deforms exactly as it was observed during a test.
In order to get the RS deformation (see Fig. 1), on each image, it is necessary to extract the edge profile of the specimen. To this aim, an automatic edge detection algorithm, implemented in MATLAB®, is used. The position of each pixel of the edge is followed through the images sequence. This allows to get the displacement (or velocity) time histories to assign as boundary conditions to the nodes of the RS.

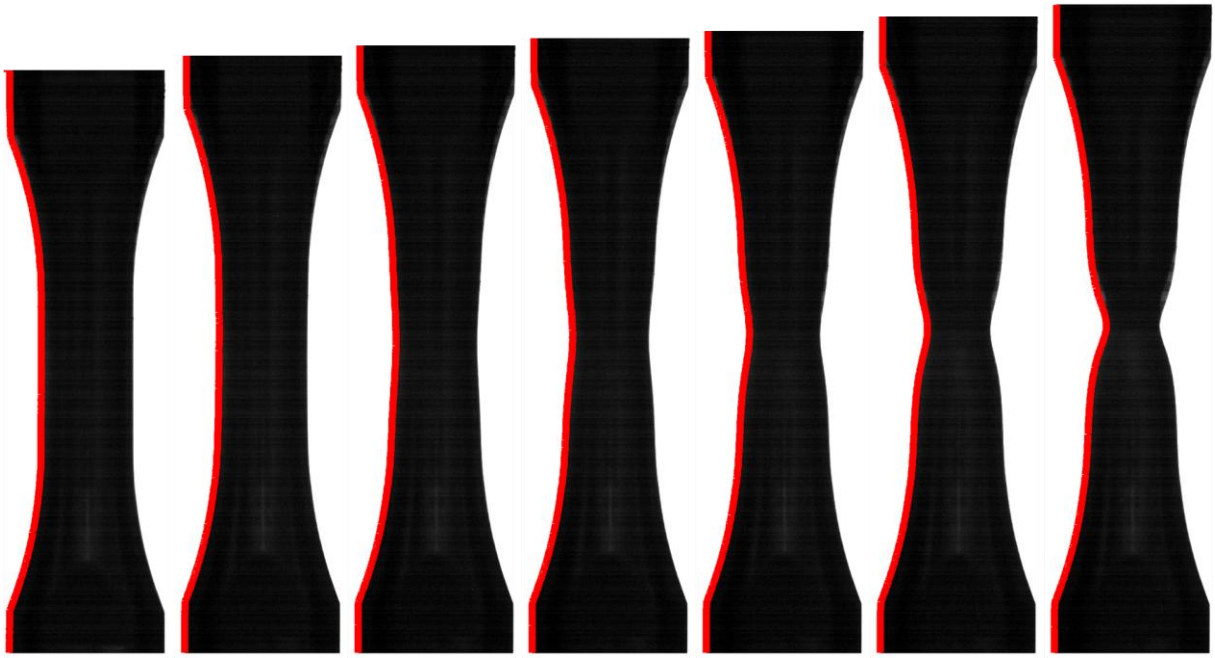

Fig.1: Digital image elaboration for the edge identification (shape profile in red).

3.1 Numerical model

In this work, the methodology is applied to the simulation of a tensile test performed on a cylindrical dog-bone specimen (gage length 5 mm, gage diameter 3 mm). It is important to underline that the same methodology could be applied to different loading conditions, such as test at different temperatures or strain-rates or more complicated tests: the requirements are the capabilities of building the FE model representing the experimental loading condition and the recording of the deformation process.
Due to the specimen geometry, the numerical model is built by using 2D axis-symmetric elements. The sketch of the model is reported in Fig. 2.
For simplicity, the analysis is performed on the experimental results obtained from a quasi-static test (the strain-rate applied to the specimen is 10^{-3} s^{-1}) at room temperature. The mechanical behavior of the material is modeled by using the MAT_015 (Johnson-Cook) constitutive equation. In accordance with the loading condition, only the hardening part of the model is considered:

$$\sigma = A + B \cdot \varepsilon_{pl}^{n} \tag{1}$$

which expresses the relation between equivalent stress and equivalent plastic strain through three parameters (*A*, *B* and *n*), which have to be determined.

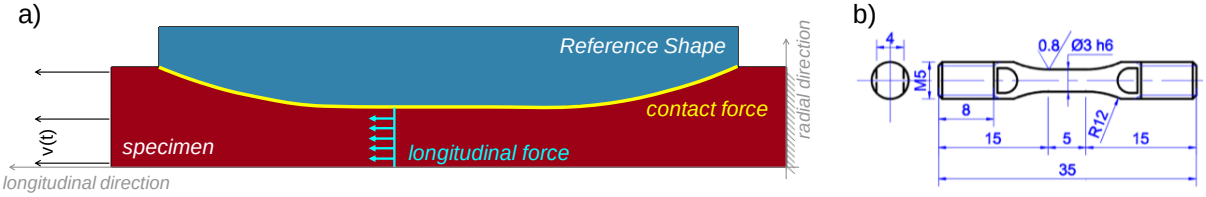

Fig.2: a) Advanced FE model used in the numerical inverse optimization; b) sketch of the specimen.

In more detail, the tensile action is obtained by imposing to one end of the specimen a time velocity profile (in accordance with data recorded from the experimental test), while the other end is fixed. This produces a longitudinal force inside the specimen which depends on the material response. This quantity is monitored by numerically computing it in one section of the specimen (far from the imposed boundaries).
The RS part is modelled with elastic elements and displacement time histories are imposed, both in longitudinal and radial direction, to each nodes as BOUNDARY_PRESCRIBED_MOTION.
The contact algorithm (2D_AUTOMATIC_CONTACT_NODE_TO_SURFACE), defined between the two parts, is such that it controls the penetration between the nodes of the RS into the surface of the specimen. The contact force represents an appropriate quantity for the evaluation of the goodness of the deformation: it is null when the specimen deforms exactly as the RS and grows up when the RS penetrates the specimen. On the other hand, if the motion is correctly applied to the RS and under the hypothesis of volume conservation (which is true for the numerical model during plastic deformation), it is not possible that the two components are completely separated, and consequently the contact force goes to zero, for a solution different from the correct one. However, particular attention has to be done to the magnitude of the contact force. As a matter of fact, greater the contact force, more significant its influence on the longitudinal force inside the specimen. Obviously, if the introduction of the RS implies a significant modification of the longitudinal response of the specimen, the simulated loading condition is far from the experimental one. Consequently, the optimization process is bad conditioned. To limit the modifications introduced by the RS, the stiffness of the contact has to be kept as low as possible: this means that the penalty factor of the contact has to be limited. Due to the non-linearity of the contact algorithm, this aspect is not so simple to be treated, since, for example, an ad-hoc evaluation has to be performed depending on the magnitude of the longitudinal material response.
Supposing to be able to properly limit the contact force, the built FE model allows to perform the numerical inverse optimization (Single Case) with two objectives (Multi-Objective Optimization, MOO): one is the minimization of the error between the experimental and the computed longitudinal force vs. stroke curves and the second one is the minimization of the contact force between the specimen and the RS. The aim of the MOO approach should be to guarantee that the set of parameters obtained is suited to simultaneously reproduce the flow stress of the material as well as the evolution of the specimen deformation.

4 Application of the methodology

The above described procedure is here applied to the material model identification for two materials: T91 steel and HDHC pure copper.
For each material, two optimizations are performed: one following the standard approach, which implies the comparison in terms of force and stroke (*"w/o shape control"*), and the other one adding the minimization of the contact force (*"w shape control"*). In the first one, the contact algorithm is not activated.
The two methods are compared in terms of computed and target longitudinal force vs. stroke response and in terms of optimized J-C models. In addition, the comparison in terms of RS and specimen deformation at different time steps is performed both qualitatively and quantitatively, by calculating the Root Mean Square Error (RMSE) between the coordinates of the nodes of the two parts of the model.

4.1 T91 steel

The high chromium ferritic/martensitic T91 steel (9% Cr, 1% Mo) shows high radiation damage and swelling tolerance as well as good resistance to high temperature creep and corrosion. For these reasons, it is widely used in the nuclear reactor sector.
In Fig. 3.a the experimental mechanical response in terms of force vs. stroke curve is shown and compared to those obtained from the optimization processes. As it is possible to notice, the material responses are very close and they well represent the experimental curve. The estimation of the discrepancy between target and computed curves is made in terms of relative Root Mean Square Error (rRMSE) and reported in Table 1: the introduction of the second objective produces a slight increase of the error in the fitting of the force vs. stroke curve. The dashed vertical line represents the initiation of the necking (maximum of the force). Nevertheless, the comparison in terms of equivalent stress vs. equivalent plastic strain curves shows that the two methodologies converge to very close J-C models (see Fig. 3.b), of which the optimized parameters are reported in Table 1.

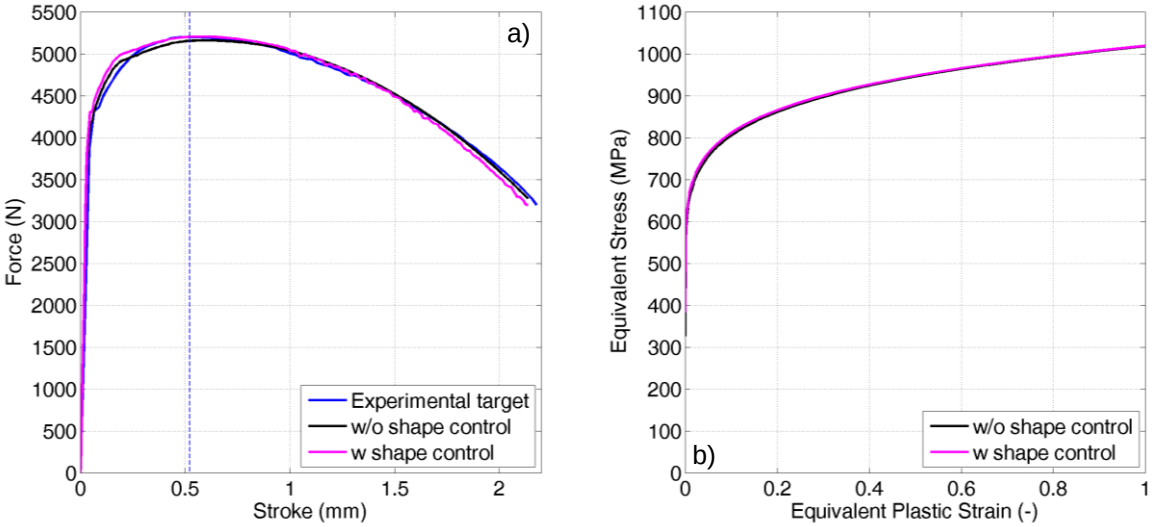

Fig.3: a) Comparison between computed (with and without shape control) and experimental force vs. stroke curves; b) comparison in terms of optimized J-C (hardening part) models for T91 steel tested at 10^{-3} s^{-1} and 25 °C.

	Parameter (units)			rRMSE (%)
Case	***A* (MPa)**	***B* (MPa)**	***n* (-)**	
w/o shape control	327	692	0.160	0.82
w shape control	384	363	0.172	1.33

Table 1: J-C parameters obtained by performing numerical optimizations with and without the specimen shape control for T91 steel.

In Fig. 4, the qualitative comparison of the deformed profiles of specimen and RS are reported at different time steps. The sequence for the case without shape control (RS is blank) refers to the simulation performed by using the optimized parameters obtained if the control of the shape is not considered, while the sequence for the case with shape control represents the result of the optimization with the control of the specimen shape. The sequence of deformed shapes for the case without shape control exclusively depends from the set of parameters used and no contact algorithm is applied: the RS is shown only to highlight, if there are, some differences between the two simulations.

A more quantitative evaluation of the differences in the deformation is performed by calculating, in the gage length area, the RMSE between the coordinates of the nodes of specimen and RS during the deformation (see Fig. 5.a). At the beginning of the test, the specimen deformation is the same by using both the sets of parameters. On the other hand, when the necking becomes significant, the error computed in case "*w/o shape control*" grows up. Looking at the diagram, it is possible to notice that the initial error is equal to about 2 μm, which represents the observational error. The fact that the average error calculated for the case "*w shape control*" is equal to this limit means that the optimization process produce the best possible result.

In Fig. 5.b the computed equivalent stress vs. equivalent plastic strain curve of three elements of the specimen are reported (simulation with shape control). The elements are longitudinally distributed starting from the centre of the necking region through the head of the specimen: the points P1 and P2 correspond to the centre and to the end of the gage length, respectively, while P3 is far from central part of the specimen. As expected, the non-uniform distribution of the mechanical quantities (plastic strain and Von Mises stress) inside the specimen can be observed. At the beginning of the test, the strain is uniformly distributed along the entire sample and also in correspondence of the point P3 the specimen is slightly deformed. When the strain localization occurs, P1 continues to deform while in P2 and P3 the deformation stops.

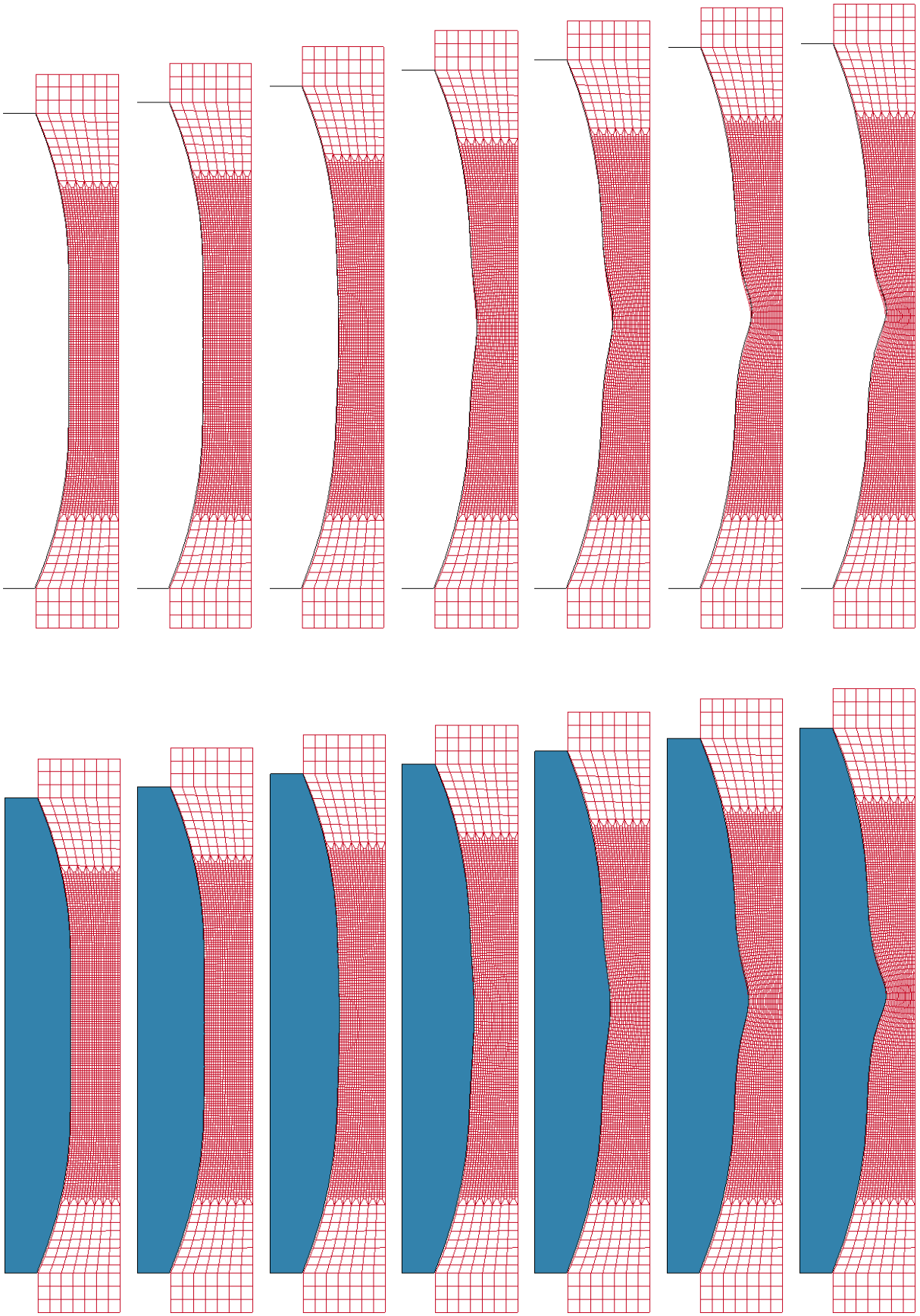

Fig.4: Sequences of the specimen deformation obtained from the two optimization strategies: without (top) and with (bottom) control of the shape for T91 steel.

Thus, for T91 steel, the advanced optimization procedure here proposed leads to an optimum which fulfils both the objectives and allows to slightly increase the reliability of the material model. In any case, the advanced procedure can be used to validate the goodness of the optimized result.

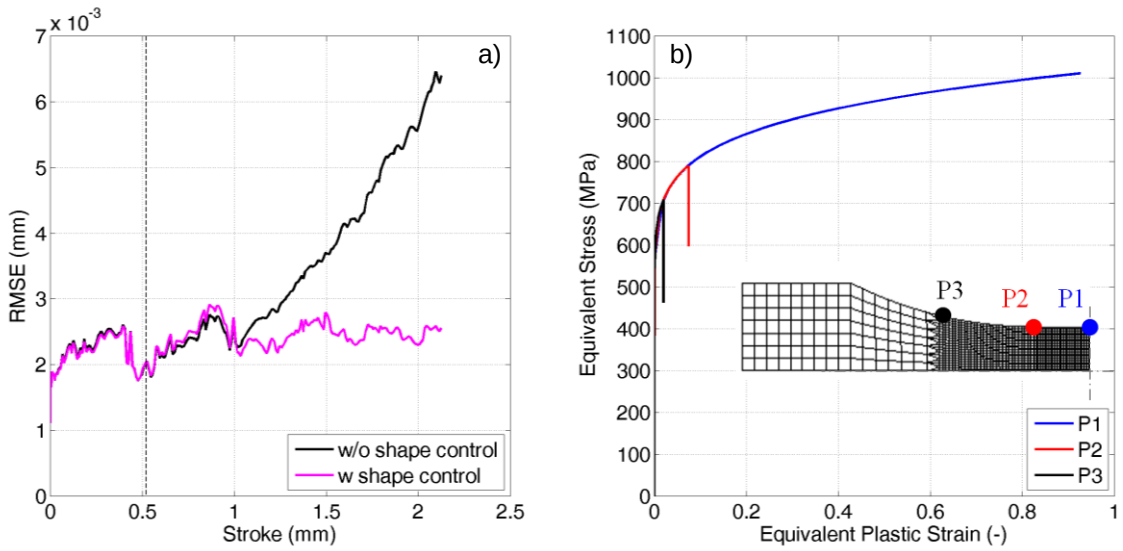

Fig.5: a) Root Mean Squared Error of the node coordinates for the two optimization methodologies as a function of the stroke (the dashed line represents the stroke at which the necking starts); b) Equivalent stress vs. equivalent plastic strain curves in three different points of the specimen (T91 steel).

4.2 HDHC copper

The same analysis is performed on HDHC pure copper. In Fig. 6.a the experimental mechanical response in terms of force vs. stroke curve is reported. The curve is compared to those obtained from the optimization processes.

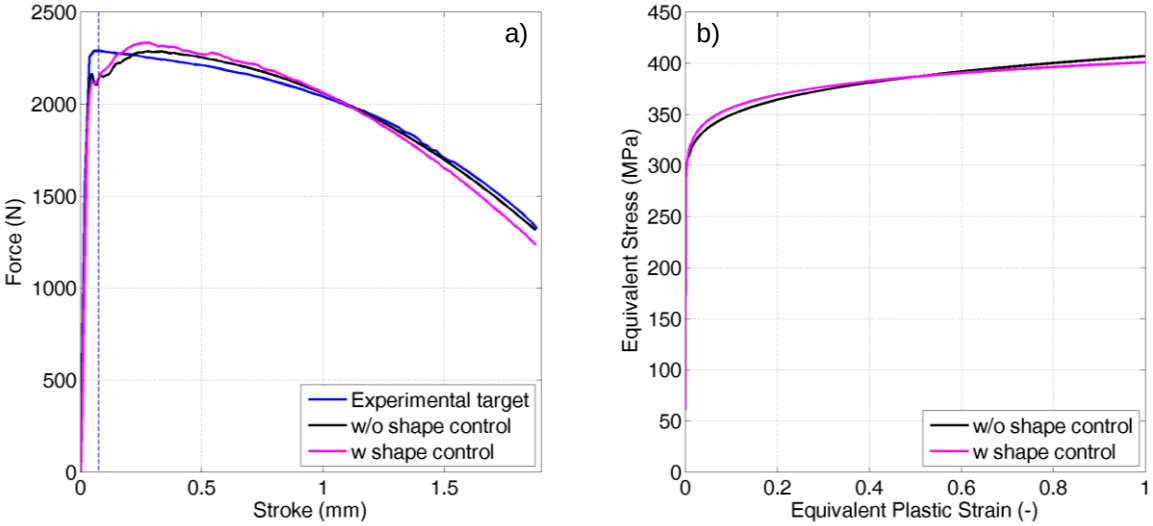

Fig.6: a) Comparison between computed (with and without shape control) and experimental force vs. displacement curves; b) comparison in terms of optimized J-C (hardening part) models for copper tested at 10^{-3} s^{-1} and 25 °C.

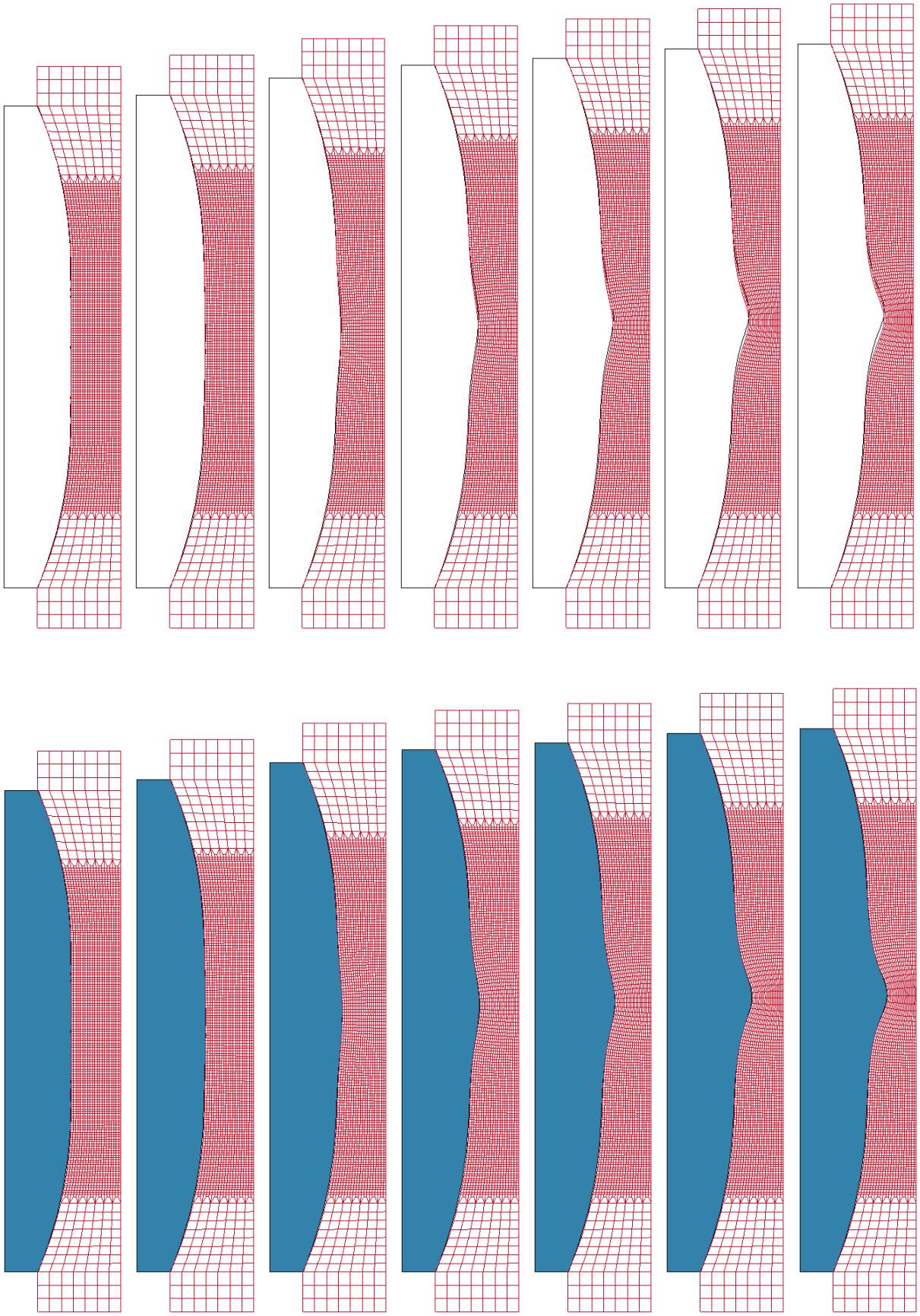

Fig.7: Sequences of the specimen deformation obtained from the two optimization strategies: without (top) and with (bottom) control of the shape for copper.

With respect to the results obtained for T91, it is possible to notice that the J-C model seems to be less suitable to reproduce the experimental curve, especially for low values of stroke. As a matter of fact, the rRMSE (relative RMSE, see Table 2) is quite high also in the single-objective optimization, and as expected, it increases in the multi-objective case. Nevertheless, both the methodologies converge to satisfactory results. The comparison in terms of equivalent stress vs. equivalent plastic strain curves shows that the two methodologies converge to slightly different J-C models (see Fig. 6.b), of which the optimized parameters are reported in Table 2.

	Parameter (units)			rRMSE (%)
Case	***A* (MPa)**	***B* (MPa)**	***n* (-)**	
w/o shape control	249	158	0.196	2.43
w shape control	61	340	0.0611	3.68

Table 2: J-C parameters obtained performing numerical optimizations with and without the specimen shape control for copper.

In Fig. 7, the qualitative comparison of the deformed profile of specimen and RS is reported at different time steps. A more quantitative evaluation of the differences in the deformation is performed by calculating, in the gage length area, the RMSE between the coordinates of the nodes of specimen and RS during the deformation (see Fig. 8.a). Also in this case, the error computed for the case "*w/o shape control*" grows up when the necking becomes significant: the discrepancy between the two simulations is higher in case of copper than in case of T91. Looking at the diagram, it is possible to notice that for copper the observational error is equal to about 1 μm. In Fig. 8.b the non-uniform distribution of the mechanical quantities (plastic strain and Von Mises stress) inside the specimen can be observed. Thus, for copper, the advanced optimization procedure here proposed leads to an optimum which fulfils both the objectives and allows to increase the reliability of the material model.

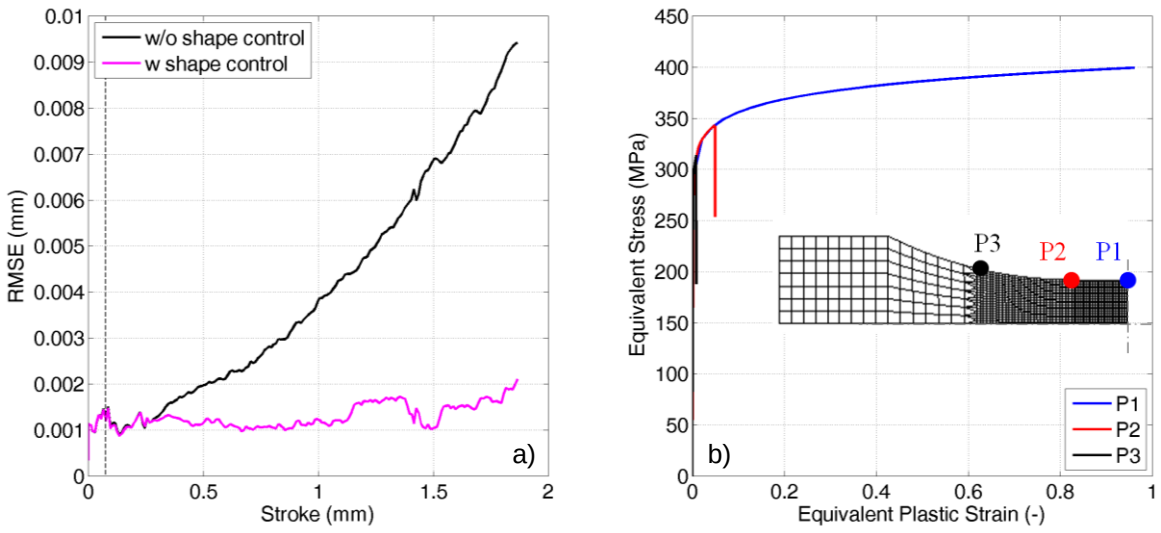

Fig.8: a) Root Mean Squared Error of the node coordinates for the two optimization methodologies as a function of the stroke (the dashed line represents the stroke at which the necking starts); b) Equivalent stress vs. equivalent plastic strain curves in three different points of the specimen (HDHC copper).

5 Summary

In this work an advanced identification procedure for material model parameters based on image analysis is presented. The methodology allows to take under control the deformation of the specimen during the optimization of the material model parameters via numerical inverse procedure based on FE simulations. This comes from the observation that the standard method does not guarantee that the deformation of the specimen corresponds to the experimental one.
The requirements for the application of the advanced technique are the measuring of mechanical response of the material in terms of force vs. stroke curve and the recording of the deformation of the specimen, which are the two objectives of the Multi-Objective Optimization. The first one is the standard objective usually used in the material model identification. The second one requires an accurate digital image elaboration and, consequently, to find a suitable strategy to impose this constraints to the FE model. In this work, the authors solve the problem by simulating ad additional component, which imposes the reference shape to the specimen.
The technique is applied to quasi-static tests of T91 steel and pure copper in case of Johnson-Cook model. In both the cases, the solution obtained with the standard methodology is in good agreement with the experimental observation, but in any case, the advanced technique allow of better tuning the solution.

6 Literature

[1] P. W. Bridgman, McGraw-Hill, New York, 1952, 9-37
[2] Zhang Z.L., Hauge M., Odegard J., Thaulov C.: " International Journal of Solids and Structures", 36, 1999, 3497-3516
[3] Tushida N., Inoue T., Enami K.: "Materials Transaction", 53(1), 2012, 133-139
[4] Villamosa V., Clausen A.H., Hopperstad O.S., Børvik T., Skjervold S.: “EPJ Web of Conference”, 26, 2012
[5] Hortigón Fuentes B., Nieto García E.J., Herrera Garrido M.A.: “Procedia Engineering”, 63, 2013, 430-437
[6] La Rosa G., Mirone G., Risitano A.: “Metallurgical and Materials transaction A”, 34°, 2003, 615-624
[7] Mirone G.: “International Journal of Solids and Structures”, 41, 2004, 3545-3564
[8] Grédiac M., Pierron F.: “International Journal of Plasticity”, 22, 2006, 602-627
[9] Rossi M., Pierron F.: “Computational mechanics”, 49(1), 2012, 53-71
[10] Kim J.H., Serpantié A., Barlat F., Pierron F., Lee M.G.: “International Journal of Solids and Structures”, 50, 2013, 3829-3842
[11] Coppetiers S., Cooreman S., Sol H., Van Houtte P., Debruyne D. : Journal of Materials Processing technology”, 211, 2011, 545-552
[12] Avril S., Pierron F., Sutton M.A., Yan J.: “Mechanics of Materials”, 40, 2008, 729-742
[13] Notta-Cuvier D., Langrand B., Markiewicz E. Lauro F., Portemont G.: “Strain”, 49, 2013, 22-45
[14] Khadyko M., Dumoulin S., Børvik T., Hopperstad O.S.: “International Journal of mechanical Science”, 88, 2014, 25-36
[15] Scapin M., Peroni L., Fichera C., Cambriani A.: “Journal of materials Engineering and Performance”, 23, 2014, 3007-3017
[16] Majzoobi G.H., Faraj Zadeh Khosroshahi S., Beik Mohammadloo H.: “Computational materials Science”, 49, 2010, 201-208